Hindawi Publishing Corporation
International Journal of Photoenergy
Volume 2012, Article ID 928503, 8 pages
doi:10.1155/2012/928503

Research Article

Effect of Electronegativity and Charge Balance on the Visible-Light-Responsive Photocatalytic Activity of Nonmetal Doped Anatase TiO_2

Jibao Lu,[1] Hao Jin,[2] Ying Dai,[1] Kesong Yang,[3] and Baibiao Huang[1]

[1] *School of Physics, State Key Laboratory of Crystal Materials, Shandong University, Jinan 250100, China*
[2] *Advanced Materials and Process Engineering Laboratory, The University of British Columbia, Vancouver, BC, Canada V6T 1Z4*
[3] *MEMS Department, Duke University, Durham, NC 27708-0300, USA*

Correspondence should be addressed to Ying Dai, daiy60@sdu.edu.cn

Received 4 July 2011; Accepted 8 August 2011

Academic Editor: Jinlong Zhang

The origin of visible light absorption and photocatalytic activity of nonmetal doped anatase TiO_2 were investigated in details in this work based on density functional theory calculations. Our results indicate that the electronegativity is of great significance in the band structures, which determines the relative positions of impurity states induced by the doping species, and further influences the optical absorption and photocatalytic activities of doped TiO_2. The effect of charge balance on the electronic structure was also discussed, and it was found that the charge-balance structures may be more efficient for visible light photocatalytic activities. In addition, the edge positions of conduction band and valence band, which determine the ability of a semiconductor to transfer photoexcited electrons to species adsorbed on its surface, were predicted as well. The results may provide a reference to further experimental studies.

1. Introduction

Titanium dioxide (TiO_2) is one of the most promising materials due to its low-cost, nontoxic, long-term stability and high oxidative power, which can be used in a wide range of technical fields, such as photocatalytic degradation of pollutants and photoelectrochemical conversion of solar energy [1, 2]. However, because of its large band gap (3.0–3.2 eV), TiO_2 is only responsive to ultraviolet irradiation ($\lambda < 378$ nm), which only accounts for ca.4% of sunlight. In order to extend the photo response of TiO_2 into the visible region and enhance its photocatalytic activity, a great deal of effort has been made to lower its threshold energy for photoexcitation as well as improve the electronic properties of TiO_2. One of the effective strategies is doping TiO_2 with nonmetallic elements, such as N [2–10], C [11–14], S [15–19], and B [20–23], all of which showed considerable photocatalytic activity under visible light.

While most researchers focus on the phenomena of redshift induced by special species doping, a thorough and systematical analysis of the modification mechanism of TiO_2, especially the essential reasons of causing various electronic structures doped with different nonmetallic elements, do not catch due attention of scientists. To explore a common rule of the band structure modification for nonmetal doping, we systematically compared the doping effects of four nonmetal species (B, C, N, and F) on anatase TiO_2. For easy comparison, we only considered the electronic properties of structures with substitutional nonmetal X (X = B, C, N, and F) to O in this paper, though the formation energies were also calculated to reveal the relative stabilities of the doped structures. To check the influence of charge balance, we have calculated the electronic structures of codoped TiO_2 with N : H, C : 2H, and B : 3H, respectively (note that the oxygen vacancies, which are not considered here, may also form to compensate the unbalanced charge, which can induce deep defect levels in the band gap [24] and usually lead to increment of the recombination). In addition, the role of the electronegativity of doping species in the optical absorption and photocatalytic activity of anatase TiO_2 was

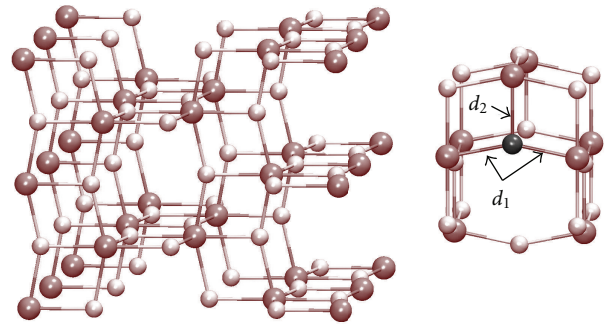

Figure 1: The supercell geometry and the doped position of the anatase TiO_2 model. The big gray ball represents Ti atom; the small light ball represents O atom; the dark ball denotes the dopant.

elucidated in this paper, and we have found that the impurity states move further away from the valence band maximum (VBM) with the increment of the electronegativity difference between the substitutional elements and oxygen. Also, the edge positions of conduction band (CB) and valence band (VB) for doped anatase TiO_2 were predicted, which should serve as a reference to future experimental studies.

2. Computational Details

Our theoretical study was carried out in the framework of density functional theory (DFT) within generalized gradient approximation (GGA) [27]. The Vienna *ab initio* Simulation Package [28, 29] (VASP) was implemented in the calculations, in which the plane-wave basis set, Vanderbilt ultrasoft pseudopotentials and the exchange-correlation functional of Perdew et al. (PBE) were used [30]. The underestimation of band gap by DFT calculations does not affect the analysis, since we only care about the relative changes of the gap, and the PBE functional has been demonstrated to be reliable by previous studies [31]. We simulated the nonmetal-doped TiO_2 model using a 48-atom supercell, in which one O atom is substituted by one impurity atom, and this corresponds to an impurity concentration of about 2%, namely, $TiO_{2-x}D_x$ with $x = 0.063$, (where D is the corresponding dopant). The supercell geometry and the doped position of the anatase TiO_2 system are shown in Figure 1. The cutoff energy for the basis set was chosen to be 500 eV, and the surface Brillouin zones were sampled at $2 \times 2 \times 2$ Γ-centered k-points [32]. The density of state (DOS) for the bulk TiO_2 was performed at the equilibrium volume using the tetrahedron method with Blöchl corrections for accuracy [33]. Considering that the impurity concentration is very low, the volume of supercell is kept fixed while the atomic positions are fully relaxed until that all forces are smaller than 10^{-4} eV/Å.

3. Results and Discussion

3.1. Electronegativity Effect on the Electronic Structures. As we know, electronegativity is the intrinsic property which measures the escaping tendency of electrons from atomic species. Based on DFT theory, Parr and coworkers [34] have given the precise definition to the electronegativity of a neutral atom, which is the negative value of the chemical potential in the ground state:

$$\chi = -\mu = -\left(\frac{\partial E}{\partial N}\right)_v, \tag{1}$$

where E and N are the ground-state electronic energy and the number of electrons, respectively. Formula (1) can then be rewritten using differential equation:

$$\chi = -\left(\frac{\partial E}{\partial N}\right)_v = \frac{E(N+1) - E(N) + E(N) - E(N-1)}{2} \approx \frac{I + A}{2}, \tag{2}$$

where I and A represent the ionization potential (IP) and electron affinity (EA) of the atom. We can see that Formula (2) has the same expression with the Mulliken's definition of the electronegativity [35]. The electronegativities of several species calculated by Formula (2) are listed in Table 1.

Table 1: EA, IP, and calculated electronegativity for several species. Unit is eV.

	EA[a]	IP[b]	Electronegativity
Ti	0.207	6.820	3.51
B	0.280	8.298	4.29
S	2.077	10.360	6.22
C	1.267	11.260	6.26
H	0.766	13.598	7.18
N	−0.072	14.534	7.23
O	1.461	13.618	7.54
Cl	3.614	12.967	8.29
F	3.398	17.422	10.41

[a]Reference [25].
[b]Reference [26].

When the nonmetallic elements are brought to the bulk TiO_2, charges will redistribute until the electrochemical potentials of the compound reach equilibrium. To unravel the inherent relationship of the electronic properties induced by different doping species, which possessed unique electronegativity, the total density of state (TDOS) and projected density of state (PDOS) for the doped TiO_2 are calculated and displayed in Figure 2. For comparison, the TDOS and

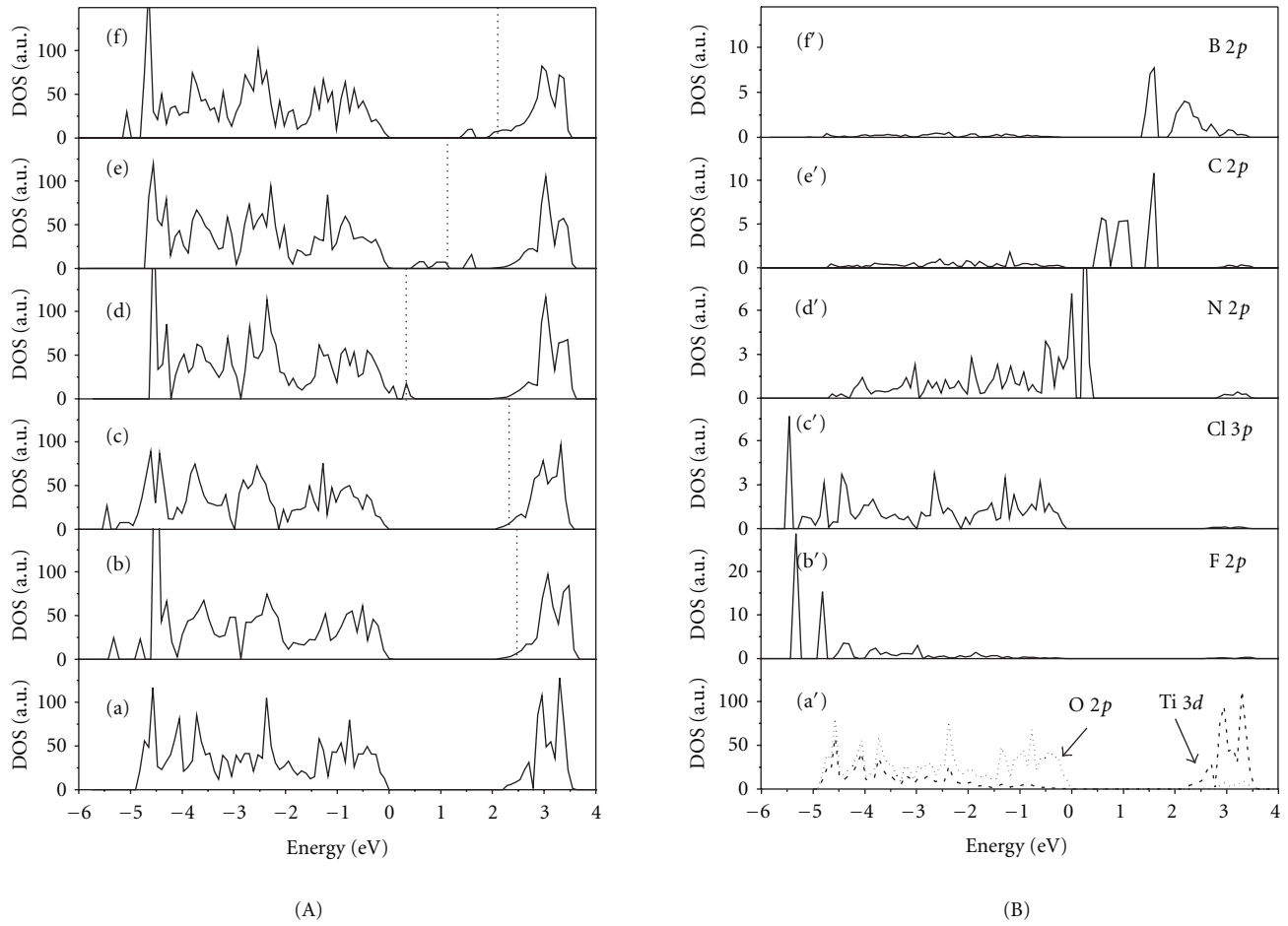

Figure 2: Total densities of states (A) and projected densities of states (B) for (a) pure anatase TiO_2, (b) F-doped TiO_2, (c) Cl-doped TiO_2, (d) N-doped TiO_2, (e) C-doped TiO_2, and (f) B-doped TiO_2. The vertical dash line defines the highest occupied level.

PDOS of pure anatase are also calculated and shown in Figures 2(a) and 2(a′). We can see that the edge of the valence band is mainly contributed by the O 2*p* atomic orbitals with a large bandwidth of about 5.0 eV, whereas the conduction band is almost entirely composed of empty Ti 3*d* orbitals.

For the F-doped TiO_2, (see Figures 2(b) and 2(b′)), the replacement of one O atom with one F atom exerts little effect on the band-gap narrowing. The impurity states introduced by F 2*p* atomic orbitals locate mainly in the lower energy range (from −5.5 eV to −4.5 eV) of the valence band, which implies that only the substitutional F to O cannot lead to any significant shift in the fundamental absorption edge of TiO_2, consistent with the former experimental results [36, 37]. It is noticed that the electronegativity mainly determines the properties of the outermost atomic orbitals, which simultaneously influence the impurity states induced by F doping. Hence, the larger electronegativity of fluorine (Table 1) should be responsible for the lower energy range of the impurity states in the valence band.

Similar doping effects also appear in Cl-doped sample. Because the electronegativity of chlorine is just a little larger than that of oxygen, they have the similar power of attracting electrons. Accordingly, the impurity states induced by Cl 3*p* states should mix with the O 2*p* states in the valence band. The calculated DOS provides evidence for the distribution character of these states. From Figures 2(c) and 2(c′), we can see clearly that the band gap reduces little as compared with the pure anatase TiO_2, and the Cl 3*p* states lie in the whole valence band, (from −5.5 eV to −0.1 eV), showing strong delocalization characteristic of Cl^- ion.

For substitutional N to O anatase model (see Figures 2(d) and 2(d′)), due to the closer electronegativity of N to that of O, the oxidative power of N is similar to that of O element. Accordingly, the N 2*p* states locate just above or in the VBM. Since some of the impurity states overlap and mix with the VBM, new edge of valence band can be formed instead of pure O 2*p* atomic orbitals, which shifts towards the higher energy and results in the band gap narrowing of about 0.43 eV. Consequently, the decrease of the photo-excitation energy leads to the redshift of absorption and extends the photo response into visible region. These results are in good agreement with previous experimental studies [6, 16, 17] and our former theoretical calculations [8, 18].

Figure 2(e) presents that the substitutional C to O atom in anatase TiO_2 introduces one empty and two occupied localized states in the middle of the gap, which

are contributed by the C 2*p* states. Experimentally, evidence of states within the band gap arising from these levels for C-doped titania has been found by XPS [38, 39].

In addition, the band gap between the highest O 2*p* states and the lowest Ti 3*d* states has little change as compared with the undoped TiO_2. Therefore, the observed redshift of optical absorption would be mainly attributed to the existence of impurity states in the mid gap of TiO_2. It is interesting that the electronegativity of carbon is close to that of nitrogen (see Table 1). However, these gap states are located at 0.68, 1.01, and 1.6 eV away from the VBM. We tentatively postulate that it is mainly due to the higher chemical valence of carbon than oxygen, which results in the shift of C 2*p* states towards the CB.

For the case of B-doped TiO_2, the substitution of B for O induces some new impurity gap states, which are dominated by the B 2*p* atomic orbitals. In addition, since the electronegativity of boron is much smaller than that of oxygen but approaches to that of titanium, the redox potentials of boron will be close to that of titanium as compared with oxygen, which leads to the impurity gap states lying below or overlapping with the conduction band, (see Figures 2(f) and 2(f′)). It is well established that the existence of impurity states in the mid gap can lower the energy barrier in the light absorption process. Therefore, these B 2*p* states should be responsible for the improvement of visible light absorption of TiO_2.

Additionally, to compare the relative stabilities of anatase TiO_2 samples doping with different elements, we calculated the formation energies as follows:

$$E_f = E_{\text{doped}} - \left(E_{\text{pure}} - \mu_O + \mu_D\right), \tag{3}$$

where E_{doped} and E_{pure} are the total energy of doped and pure anatase supercell, respectively. The symbols μ_O and μ_D represent the chemical potential of oxygen and doped elements, respectively. Here we only focus on the so-called oxygen-rich synthesis condition, where the chemical potential for oxygen is related to the chemical potential for gaseous O_2 at 1 bar. We report our results in Table 2 with the optimized Ti-D bond lengths also listed. It can be noted that the formation energy decreases with the increase of electronegativity of dopant. In particular, for the F-doped case, the formation energy has a negative valve, which implies that it is thermodynamically preferred. In addition, it is worthwhile to mention that the substitutional (for O) doping could be much easier under oxygen-poor condition due to the lower oxygen partial pressure, while the relative stabilities between the structures doped with different ions remain the same as those under oxygen-rich condition.

3.2. Effect of Charge Balance on the Electronic Structures. To understand the effect of charge balance on the electronic structures, we balance the charge of N, C, and B with one H, two H, and three H atoms, respectively, which is reasonable because the doped TiO_2 materials were usually processed with amine solution [3–5], H_2 [6], or BH_3 atmosphere [20, 21]. In the calculations, one O atom is replaced by N : H species, C : 2H species, and B : 3H species, respectively (see Figure 3). The corresponding DOS of N : H-doped, C : 2H-doped, and B : 3H-doped TiO_2 are calculated and shown in Figure 4. Obviously, for the C-doped TiO_2, when the charge balance structure is obtained, three isolated gap states are replaced by one occupied state, which is located near the VBM, (see Figures 4(c) and 4(c′)). From Figure 4, we can see clearly that with the decrease of the electronegativity difference between oxygen and substitutional elements, (N, C, and B), the impurity states become closer to the VBM. In addition, when the charges are balanced, the electron donors (H) may contribute to the lowering of the energy levels related to the acceptors (N, C, and B), resulting in the impurity states downward to the VBM, which agrees well with the previous studies [40]. Accordingly, the N : H species may enhance the mixing of impurity states induced by N 2*p* states and O 2*p* atomic orbitals in the VBM, and finally new valence bands can be formed, which could contribute to the formation of the band-band transition, in favor of the visible-light-driven catalytic activities. When it comes to the B : 3H-codoped case, though the impurity energy level moves a little toward the VBM, the isolated states are still localized in the midgap because of the large difference of the electronegativity between substitutional boron and oxygen. Therefore, based on these understandings, we can draw a conclusion that if the electronegativity of oxygen is close to that of the doping species, together with the simultaneous formation of charge-balance structure, the doped TiO_2 may possess high photocatalytic activity under visible light.

Additionally, we also studied the N : F codoping effect on the anatase TiO_2, which are expected to be efficient to the visible light photocatalytic activity according to the analysis above. The supercell is simulated by replacing two O atoms with one N atom and one F atom, respectively (see Figure 3(d)), and the corresponding structure and DOS are shown in Figure 4(a). It is apparent that the impurity states induced by N and F doping locate in different range of the valence band, which can be ascribed to their unique electronegativities as we discussed above. Obviously, the absorption edge of new band in the visible light originated from the doped N atoms rather than doped F atoms, consistent with the former studies [36, 37]. Furthermore, the impurity states are fully filled with the electrons at the ground state, which can be attributed to the fact that the doped F^- ion compensates the charge of N^{3-} ion. Therefore, similar to the case of N : H codoping, the N : F complex results in

Table 2: Calculated bond lengths, lattice variation, and defect formation energies.

	d_1 (Å)	d_2 (Å)	$\Delta V/V$	Defect formation energies (eV)
Pure	1.990	1.926		
B-doped	2.650	2.118	6.6%	7.08
C-doped	2.217	2.010	5.1%	5.94
N-doped	2.043	1.957	4.8%	5.04
Cl-doped	2.519	2.224	6.6%	3.43
F-doped	2.227	2.043	4.9%	−0.85

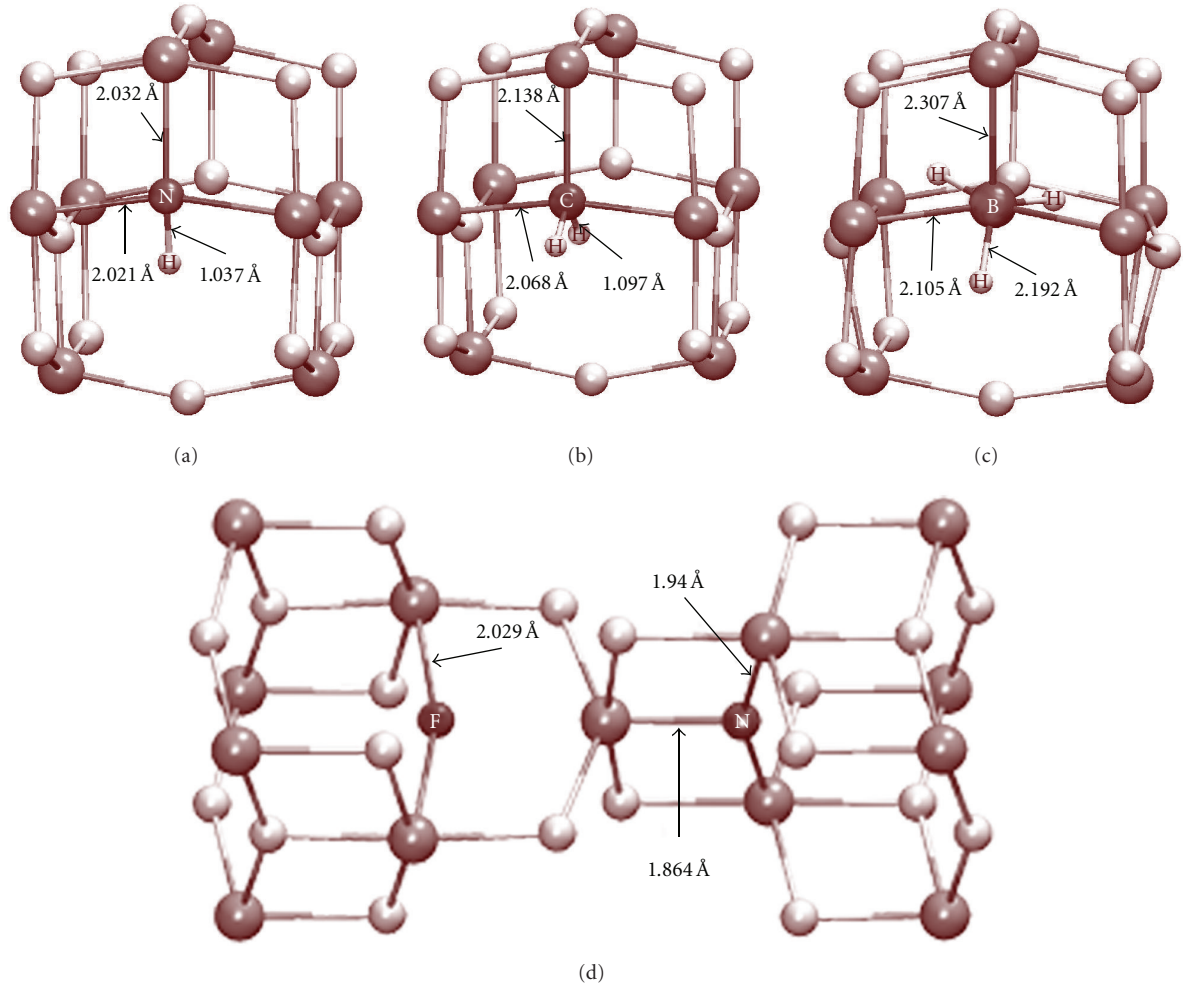

Figure 3: The optimal structures for (a) N : H-doped TiO_2, (b) C : 2H-doped TiO_2, (c) B : 3H-doped, and (d) N : F codoped TiO_2.

the formation of the charge-balance structure and could enhance the mixing of impurity states with the VBM, which favors the band-band transition and the photocatalytic activities under visible light.

3.3. Prediction of Redox Potentials from Atomic Electronegativity. As we know, the ability of a semiconductor to transfer photoexcited electrons to species adsorbed on its surface is governed by the band energy position of the semiconductor and the redox potentials of the adsorbate, which is related to the electronegativity [1]. Therefore, to thoroughly understand the effects of the electronegativity on the doped TiO_2, we have calculated the positions of CB and the VB edge using the concept of the semiconductor electronegativity, which is defined as the geometric mean of the electronegativities of the constituent atoms:

$$\chi(S) = \sqrt[N]{\chi_1^n \chi_2^s \cdots \chi_{n-1}^p \chi_n^q}, \tag{4}$$

where χ_n, n, and N are the electronegativity of the constituent atom, the number of species, and the total number of atoms in the compound, respectively [41].

The CB edge position of a semiconductor at the point of zero charge (E_{CB}^0) can be expressed empirically by

$$E_{CB}^0 = \chi(S) - E^e - \frac{1}{2}E_g, \tag{5}$$

where E_g and E^e are the band gap energy of the semiconductor and the energy of free electrons on the hydrogen scale (~4.5 eV) [42]. Although this method cannot give precise absolute values due to the neglect of structural factors, it may give a rough estimate of the relative positions of normal hydrogen electrode (NHE), which could provide a reference to future experimental studies.

Due to the well-known drawback of DFT theory, our DFT calculations under GGA level give band gaps of about 2.2 eV, smaller than the experimental values (3.23 eV) [43]. In order to correct the underestimation of band gaps, we employed scissor operator, that is, a systematic upward shifting of the unoccupied states by a constant amount. In addition, we postulate that the amount of the band gaps underestimation would not be affected by doping effect because long-range screening properties of doped TiO_2 are expected to be similar to those in pure TiO_2. Therefore, in this paper

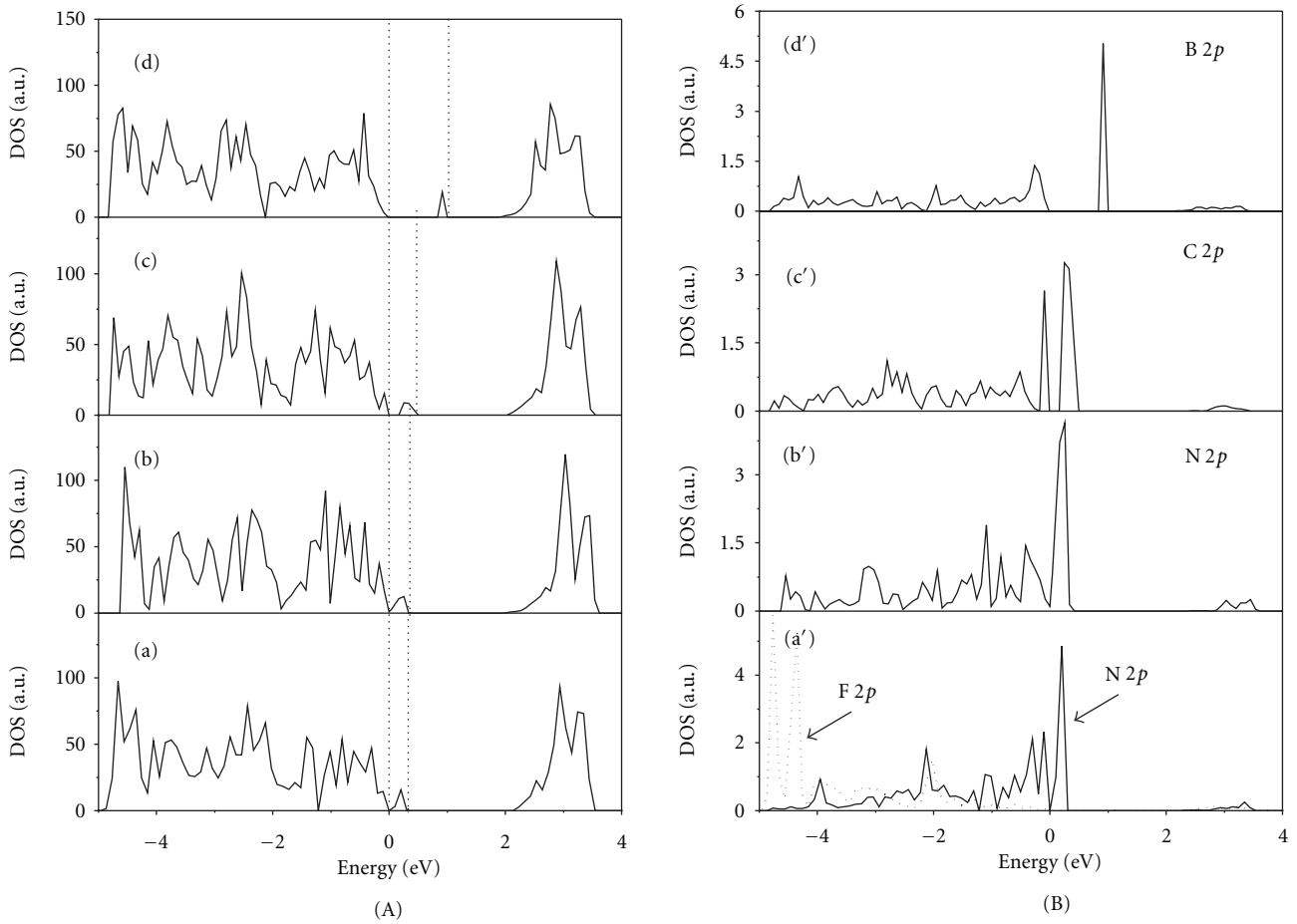

Figure 4: Total densities of states (A) and projected densities of states (B) for (a) N : F codoped TiO_2, (b) N : H-doped TiO_2, (c) C : 2H-doped TiO_2, (d) B : 3H-doped TiO_2. The vertical dash line defines the highest occupied level.

we use a rigid constant shift of the band gaps for both pure and doped TiO_2, namely, 1.03 eV. Consequently, the adjusted band gaps are 3.23 eV for pure TiO_2, which is in line with the experimental values.

According to the strategies mentioned above, the rough CB edge potential of pure anatase TiO_2 is −0.27 eV with respect to NHE. Subsequently the VB edge position is determined as 2.96 eV based on its band gap energy. The corrected band gap energy (E_g) and the corresponding CB and VB edge positions versus NHE are shown in Figure 4.

It can be found that the electronegativity of doping species produces certain influence on the oxidative potential of doped TiO_2. Generally, when the impurity states locate in the lower range of the valence band or mixing with the VBM, (see Figures 5(b)–5(g)), the doped TiO_2 possess more oxidative power with the increasing of the electronegativity of the doping species or complex. When it comes to the B : H-codoped, C- and B-doped cases, these materials also obey such rule, (see Figures 5(h)–Figure 5(k)). However, since there are some isolated states in the midgap, the situations may become more complicated, which need further studies. Moreover, it can be known from the results that though F-doping could not contribute to the optical absorption spectra, it possesses strong oxidative potential, which could enhance the redox ability of TiO_2. In addition, it has been studied that the doped F atoms could reduce the electron-hole recombination rate and further enhances the photocatalytic activity [36, 44]. Therefore, the N : F-codoped TiO_2 may possess high-photocatalytic activity under visible light irradiation, which makes it an excellent candidate for further applications.

Finally, since surface conditions are of key importance in heterogeneous photocatalysis, a further discussion on how the findings can be applied to doped surfaces is necessary. On the pure TiO_2 surfaces, additional surface states will be introduced in the electronic structures due to the surface reconstruction or dangling bonds formed on it, whereas for the deep inner layers below surfaces the electronic structure retains its bulk character. So that the above findings can be rationally applied to the doping of inner layers of surfaces, while when they are applied to the doping of the several outermost layers of surfaces, additional calculations and analysis are needed to give a verification.

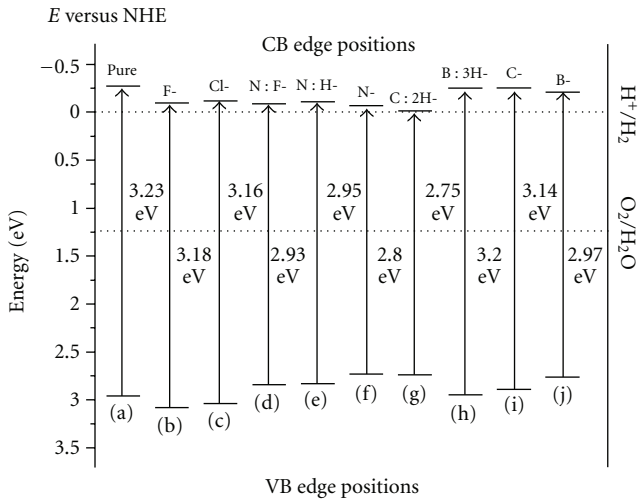

Figure 5: Calculated edge positions of conduction band and valence band for pure and nonmetal doped anatase TiO_2.

4. Conclusions

Our results show that when the electronegativity of the doping species is larger than that of oxygen, such as F and Cl, the impurity states induced mainly by outermost atomic orbitals locate in the lower energy range of the valence band, which cannot contribute to the redshift of absorption. Whereas when the electronegativity of the doping species is smaller than that of oxygen, the impurity states will lie above the VBM. Especially, if the difference is small, such as N, the impurity states can mix and overlap with the O 2*p* states, leading to the photo response of TiO_2 under visible light irradiation. In addition, once the charge balance structures are obtained, the electron donors can lower the impurity states levels and enhance the mixing of N 2*p* atomic orbitals with O 2*p* states. Also, we have found that the N:F complex may be more efficient to the visible light photocatalytic activities. Hence, on the basis of these understandings, we have proposed a new way to interpret the mechanism of the redshift and predict the photocatalytic activities doping with different species. Furthermore, based on the definition of the semiconductor electronegativity, the CB and VB edge positions have been predicted, which demonstrated that the doped TiO_2 possess favorable redox potentials under visible light, making them promising materials for further applications. Based on the above analysis, we conclude that a careful selection of codopants to yield a charge-balance codoped system is an effective way to improve the visible-light-responsive photocatalytic activity of nonmetal doped TiO_2.

Acknowledgments

This work is supported by the National Basic Research Program of China (973 program, Grant no. 2007CB613302), National Natural Science Foundation of China under Grant no. 11174180 and 20973102, Natural Science Foundation of Shandong Province under Grant no. ZR2011AM009.

References

[1] A. L. Linsebigler, G. Lu, and J. T. Yates, "Photocatalysis on TiO_2 surfaces: Principles, mechanisms, and selected results," *Chemical Reviews*, vol. 95, no. 3, pp. 735–758, 1995.

[2] R. Asahi, T. Morikawa, T. Ohwaki, K. Aoki, and Y. Taga, "Visible -light photocatalysis in nitrogen-doped titanium oxides," *Science*, vol. 293, no. 5528, pp. 269–271, 2001.

[3] C. Burda, Y. Lou, X. Chen, A. C. S. Samia, J. Stout, and J. L. Gole, "Enhanced nitrogen doping in TiO_2 nanoparticles," *Nano Letters*, vol. 3, no. 8, pp. 1049–1051, 2003.

[4] A. V. Emeline, V. N. Kuznetsov, V. K. Rybchuk, and N. Serpone, "Visible-light-active titania photocatalysts: the case of n-doped TiO_2s—properties and some fundamental issues," *International Journal of Photoenergy*, vol. 2008, Article ID 258394, 19 pages, 2008.

[5] B. Wawrzyniak, A. W. Morawski, and B. Tryba, "Preparation of TiO_2-nitrogen-doped photocatalyst active under visible light," *International Journal of Photoenergy*, vol. 2006, Article ID 68248, 8 pages, 2006.

[6] L. Miao, S. Tanemura, H. Watanabe, Y. Mori, K. Kaneko, and S. Toh, "The improvement of optical reactivity for TiO_2 thin films by N_2-H_2 plasma surface-treatment," *Journal of Crystal Growth*, vol. 260, no. 1-2, pp. 118–124, 2004.

[7] M. Batzill, E. H. Morales, and U. Diebold, "Influence of nitrogen doping on the defect formation and surface properties of TiO_2 rutile and anatase," *Physical Review Letters*, vol. 96, no. 2, Article ID 026103, 2006.

[8] C. Di Valentin, E. Finazzi, G. Pacchioni et al., "N-doped TiO_2: theory and experiment," *Chemical Physics*, vol. 339, no. 1–3, pp. 44–56, 2007.

[9] K. Yang, Y. Dai, and B. Huang, "Study of the nitrogen concentration influence on N-doped TiO_2 anatase from first-principles calculations," *Journal of Physical Chemistry C*, vol. 111, no. 32, pp. 12086–12090, 2007.

[10] S. Liu, J. Yu, and W. Wang, "Effects of annealing on the microstructures and photoactivity of fluorinated N-doped TiO_2 ," *Physical Chemistry Chemical Physics*, vol. 12, no. 38, pp. 12308–12315, 2010.

[11] Z. Wu, F. Dong, Y. Liu, and H. Wang, "Enhancement of the visible light photocatalytic performance of C-doped TiO_2 by loading with V_2O_5 ," *Catalysis Communications*, vol. 11, no. 2, pp. 82–86, 2009.

[12] S. U. M. Khan, M. Al-Shahry, and W. B. Ingler Jr., "Efficient photochemical water splitting by a chemically modified n-TiO_2 ," *Science*, vol. 297, no. 5590, pp. 2243–2245, 2002.

[13] S. Sakthivel and H. Kisch, "Daylight photocatalysis by carbon-modified titanium dioxide," *Angewandte Chemie*, vol. 42, no. 40, pp. 4908–4911, 2003.

[14] Y. Kesong, D. Ying, H. Baibiao, and W. Myung-Hwan, "Density functional characterization of the visible-light absorption in substitutional C-anion- and C-cation-doped TiO_2 ," *Journal of Physical Chemistry C*, vol. 113, no. 6, pp. 2624–2629, 2009.

[15] V. M. Menéndez-Flores, D. W. Bahnemann, and T. Ohno, "Visible light photocatalytic activities of S-doped TiO_2-Fe^{3+} in aqueous and gas phase," *Applied Catalysis B: Environmental*, vol. 103, no. 1-2, pp. 99–108, 2011.

[16] T. Ohno, M. Akiyoshi, T. Umebayashi, K. Asai, T. Mitsui, and M. Matsumura, "Preparation of S-doped TiO_2 photocatalysts and their photocatalytic activities under visible light," *Applied Catalysis A: General*, vol. 265, no. 1, pp. 115–121, 2004.

[17] K. Nishijima, T. Kamai, N. Murakami, T. Tsubota, and T. Ohno, "Photocatalytic hydrogen or oxygen evolution from

water over S- or N-doped TiO_2 under visible light," *International Journal of Photoenergy*, vol. 2008, Article ID 173943, 7 pages, 2008.

[18] J. C. Yu, W. Ho, J. Yu, H. Yip, K. W. Po, and J. Zhao, "Efficient visible-light-induced photocatalytic disinfection on sulfur-doped nanocrystalline titania," *Environmental Science and Technology*, vol. 39, no. 4, pp. 1175–1179, 2005.

[19] K. Yang, Y. Dai, and B. Huang, "Understanding photocatalytic activity of S- And P-doped TiO_2 under visible light from first-principles," *Journal of Physical Chemistry C*, vol. 111, no. 51, pp. 18985–18994, 2007.

[20] S. In, A. Orlov, R. Berg et al., "Effective visible light-activated B-doped and B,N-codoped TiO_2 photocatalysts," *Journal of the American Chemical Society*, vol. 129, no. 45, pp. 13790–13791, 2007.

[21] X. Nie, S. Zhuo, G. Maeng, and K. Sohlberg, "Doping of TiO_2 polymorphs for altered optical and photocatalytic properties," *International Journal of Photoenergy*, vol. 2009, Article ID 294042, 22 pages, 2009.

[22] K. Yang, Y. Dai, and B. Huang, "Origin of the photoactivity in boron-doped anatase and rutile TiO_2 calculated from first principles," *Physical Review B*, vol. 76, no. 19, Article ID 195201, 6 pages, 2007.

[23] K. Yang, Y. Dai, and B. Huang, "Density functional study of boron-doped anatase TiO_2 ," *Journal of Physical Chemistry C*, vol. 114, no. 46, pp. 19830–19834, 2010.

[24] J. Lu, K. Yang, H. Jin, Y. Dai, and B. Huang, "First-principles study of the electronic and magnetic properties of oxygen-deficient rutile $TiO_2(1\ 1\ 0)$ surface," *Journal of Solid State Chemistry*, vol. 184, no. 5, pp. 1148–1152, 2011.

[25] J. E. Huheey, *Inorganic Chemistry*, Harper and Row, New York, NY, USA, 3rd edition, 1983.

[26] J. F. Liebman, "Regularities and relations among lonization potentials of nontransition elements," *Journal of Chemical Education*, vol. 50, no. 12, pp. 831–834, 1973.

[27] J. P. Perdew and Y. Wang, "Accurate and simple analytic representation of the electron-gas correlation energy," *Physical Review B*, vol. 45, no. 23, pp. 13244–13249, 1992.

[28] G. Kresse and J. Furthmüller, "Efficiency of ab-initio total energy calculations for metals and semiconductors using a plane-wave basis set," *Computational Materials Science*, vol. 6, no. 1, pp. 15–50, 1996.

[29] G. Kresse and J. Furthmüller, "Efficient iterative schemes for ab initio total-energy calculations using a plane-wave basis set," *Physical Review B*, vol. 54, no. 16, pp. 11169–11186, 1996.

[30] J. P. Perdew, K. Burke, and M. Ernzerhof, "Generalized gradient approximation made simple," *Physical Review Letters*, vol. 77, no. 18, pp. 3865–3868, 1996.

[31] W.-J. Yin, S.-H. Wei, M. M. Al-Jassim, and Y. Yanfa, "Double-hole-mediated coupling of dopants and its impact on band gap engineering in TiO_2 ," *Physical Review Letters*, vol. 106, no. 6, Article ID 066801, 2011.

[32] H. J. Monkhorst and J. D. Pack, "Special points for Brillouin-zone integrations," *Physical Review B*, vol. 13, no. 12, pp. 5188–5192, 1976.

[33] P. E. Blöchl, O. Jepsen, and O. K. Andersen, "Improved tetrahedron method for Brillouin-zone integrations," *Physical Review B*, vol. 49, no. 23, pp. 16223–16233, 1994.

[34] R. G. Parr, R. A. Donnelly, M. Levy, and W. E. Palke, "Electronegativity: The density functional viewpoint," *The Journal of Chemical Physics*, vol. 68, no. 8, pp. 3801–3807, 1978.

[35] R. S. Mulliken, "A new electroaffinity scale; Together with data on valence states and on valence ionization potentials and electron affinities," *The Journal of Chemical Physics*, vol. 2, no. 11, pp. 782–793, 1934.

[36] D. Li, H. Haneda, S. Hishita, and N. Ohashi, "Visible-light-driven N-F-codoped TiO_2 photocatalysts. 2. Optical characterization, photocatalysis, and potential application to air purification," *Chemistry of Materials*, vol. 17, no. 10, pp. 2596–2602, 2005.

[37] D. Huang, S. Liao, S. Quan et al., "Preparation of anatase F doped TiO_2 sol and its performance for photodegradation of formaldehyde," *Journal of Materials Science*, vol. 42, no. 19, pp. 8193–8202, 2007.

[38] X. Chen and C. Burda, "Photoelectron spectroscopic investigation of nitrogen-doped titania nanoparticles," *Journal of Physical Chemistry B*, vol. 108, no. 40, pp. 15446–15449, 2004.

[39] X. Chen and C. Burda, "The electronic origin of the visible-light absorption properties of C-, N- and S-doped TiO_2 nanomaterials," *Journal of the American Chemical Society*, vol. 130, no. 15, pp. 5018–5019, 2008.

[40] L. Mi, P. Xu, H. Shen, P. Wang, and W. Shen, "First-principles calculation of N:H codoping effect on energy gap narrowing of TiO_2 ," *Applied Physics Letters*, vol. 90, no. 17, Article ID 171909, 3 pages, 2007.

[41] R. T. Sanderson, *Chemical Periodicity*, Reinhold, New York, NY, USA, 1960.

[42] S. R. Morrison, *Electrochemistry at Semiconductor and Oxidized Metal Electrodes*, Plenum Press, New York, NY, USA, 1980.

[43] J. B. Goodenough and A. Hamnett, *Landolt-Börnsterin*, vol. 3 of *New Series*, Springer, Berlin, Germany, 1984, Edited by O. Madelung.

[44] J. C. Yu, J. Yu, W. Ho, Z. Jiang, and L. Zhang, "Effects of F-doping on the photocatalytic activity and microstructures of nanocrystalline TiO_2 powders," *Chemistry of Materials*, vol. 14, no. 9, pp. 3808–3816, 2002.